

Determination of *syn/anti* Isomerism in DCNQI Derivatives by 2D Exchange Spectroscopy: Theoretical Underpinning

Fernando P. Cossío,^[a] Pilar de la Cruz,^[b] Antonio de la Hoz,^{*[c]} Fernando Langa,^[b] Nazario Martín,^{*[d]} Pilar Prieto,^[c] and Luis Sánchez^[d]

Keywords: Ab initio calculations / NMR spectroscopy / 2D EXSY / Cyanoimines

The dynamic *syn/anti* isomerism resulting from the inversion of the cyano group at the C=N double bond in a series of substituted DCNQIs has been investigated in solution by two-dimensional exchange spectroscopy (2D EXSY). The isomers formed were characterised by ¹H NMR at 223 K to slow down the inversion process of the cyanoimine group as well as by H,H COSY spectra. Whereas compounds **6**, **7**, **9** and **10** show only one isomer, compounds **8** and **11** show two isomers with two inversion processes and compounds **12** and **13** show three isomers and four inversion processes. The energy barrier for the *syn/anti* isomerization of the NCN groups has been estimated from the rate constants determined from the 2D EXSY spectra, and very close values (13.16–13.93 kcal/mol for a single inversion) were found for all compounds. Isomerizations involving two NCN groups (compounds **12** and **13**) exhibited higher activation free energy values (13.41–14.40 kcal/mol). Theoretical calculations of these free energy barriers are in excellent agreement with the experi-

mental values, especially when solvent effects are taken into account. Theoretical calculations at B3LYP/6–31G* level predict planar geometries for the DCNQI derivatives studied (**6** and **8**), in particular when solvent effects are considered. This is in perfect agreement with the experimental data. Two-electron stabilizing interactions, as well as solvent effects, are related to the relative energies of the different stereoisomers. The relative equilibrium populations of the different isomers have been calculated using semiempirical energies and Boltzmann's distribution. Although the most stable isomer as determined by AM1 method is in qualitative agreement with that deduced from NMR experiments in all DCNQI derivatives studied, better quantitative correlations are obtained at the B3LYP(L1A1)/6–31G* calculation level. Comparison of both semiempirical and ab initio calculations reveal that in these DCNQI systems AM1 is the method of choice for those larger systems whose size prevents energy calculations at higher levels.

Introduction

Organic charge-transfer (CT) complexes and CT salts have been intensively studied in search of electrically conducting and superconducting properties.^[1] Synthetic efforts in the preparation of these “organic metals” have mainly been directed to the modification of the electron donor component and, to a lesser extent, to the design of novel electron acceptors.^[2] With regard to the acceptor component, tetracyano-*p*-quinodimethane (TCNQ)^[3] (**1**) and dicyano-*p*-quinonediimine (DCNQI)^[4] (**2**) are, together with the [M(dmit)₂] complexes^[5] and the more recent [60]fullerene

derivatives,^[6] the most important, and a wide variety of derivatives have been prepared during the last few years.^[7]

TCNQ and DCNQI molecules are the subjects of renewed interest due to the growing field of conductive Langmuir–Blodgett (LB) films based on molecular conductors,^[8] their use as components of materials for molecular electronic devices,^[9] and the novel magnetic and optical properties that inter- or intramolecular CT complexes can exhibit.^[7]

The first well-known CT complex was formed by the TCNQ molecule and tetrathiafulvalene (TTF), thus opening up the field of molecular organic conductors.^[10] The most recent family of DCNQI acceptors, developed by Hünig and co-workers,^[11] presents some interesting advantages over the TCNQ predecessor. Firstly, DCNQIs are easily prepared in a one-pot procedure from the respective quinones,^[12] and secondly the acceptor strength of DCNQI is similar to that of TCNQ and can be finely tuned by the electronic effects of the substituents present on the DCNQI ring.^[13] In addition, and in sharp contrast with the TCNQ analogues, a multistep redox behaviour is observed for the laterally fused π -extended derivatives.^[14] Thirdly, in contrast to the substituted TCNQ derivatives, which are severely distorted out of planarity, most DCNQIs are planar molecules,^[15] which is a prerequisite for electrical conductivity.^[1]

^[a] Facultad de Química, Universidad del País Vasco. Apdo 1072, 20080 San Sebastián, Spain
E-mail: qopcomof@sq.ehu.es

^[b] Facultad de Ciencias del Medio Ambiente, Universidad de Castilla-La Mancha, 45001 Toledo, Spain
E-mail: flanga@amb-to.uclm.es

^[c] Facultad de Química, Universidad de Castilla-La Mancha, 13071 Ciudad Real, Spain
E-mail: adlh@qino-cr.uclm.es

^[d] Departamento de Química Orgánica, Facultad de Química, Universidad Complutense, E-28040 Madrid, Spain
E-mail: nazmar@eucmax.sim.ucm.es

Supporting information for this article is available on the WWW under <http://www.wiley-vch.de/home/eurjoc> or from the author.

This planarity has been attributed to the less sterically demanding cyanoimino group ($=N-CN$) in comparison with the most rigid dicyanomethylene group ($=C(CN)_2$) present in TCNQ derivatives.

Depending upon the substitution pattern on the DCNQI ring, these molecules can display *syn/anti* isomerism, the configuration of which has been determined by 1H NMR spectroscopy at varying temperatures.^[12]

Although both isomers are in principle possible for the parent unsubstituted DCNQI, the *anti* isomer is preferred (80:20)^[12] since the dipole moments are reduced in this configuration. Very recently, a new series of 2,3-disubstituted *N,N'*-dicyanoimines have been reported and their *syn/anti* isomers determined.^[16]

We have also reported the synthesis and redox properties of single-component donor-acceptor organic compounds composed of a DCNQI-derived strong electron acceptor and 1,4-benzoxazine (3),^[17] 1,4-benzodithiin (4)^[18] and 1,4-benzoxathiin (5)^[18] as donor fragments.

These compounds (3–5), which according to X-ray analysis and theoretical calculations are distorted from planarity, exhibit a photoinduced intramolecular electron transfer from the high-energy HOMO furnished by the donor moiety to the low-energy LUMO located on the DCNQI fragment.

Interestingly, the energy difference between planar and butterfly structures of the DCNQI moiety is calculated to be < 3 kcal/mol at the *ab initio* 6–31G* level.^[18] The assignment of hyperfine coupling constants in the EPR spectra, in agreement with the temperature-dependent 1H NMR spectra and theoretical calculations, indicate the preferred configurations shown in Scheme 1.

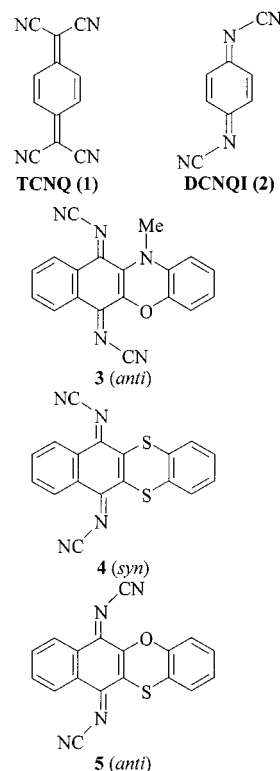
In this paper we describe a series of differently substituted DCNQIs prepared for investigation, by two-dimensional exchange spectroscopy (2D EXSY), of the multiple dynamic processes which take place in solution as a consequence of the inversion of the cyano group at the $C=N$ double bond, leading to an equilibrium between different isomers. In order to rationalise the experimental findings, theoretical calculations have also been carried out at semi-empirical (AM1 and PM3) and *ab initio* (3–21G^(*) and 6–31G^(*)) levels.

Results and Discussion

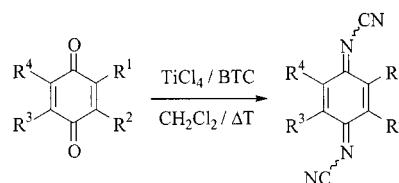
The target DCNQI derivatives were prepared from the respective quinones by reaction with bis(trimethylsilyl)carbodiimide (BTC) in the presence of titanium tetrachloride, following Hünig's procedure (Scheme 2).^[4,12] The compounds prepared are listed in Scheme 3, Scheme 4 and Scheme 5.

Dynamic Nuclear Magnetic Resonance (DNMR) Studies

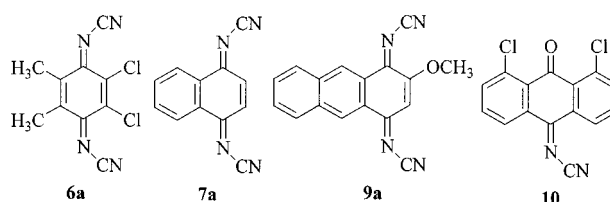
The most commonly used techniques for evaluation of reaction rates are line-shape analysis and magnetisation transfer.^[19] However, the application of both methods becomes increasingly difficult when the number of possible



Scheme 1



Scheme 2

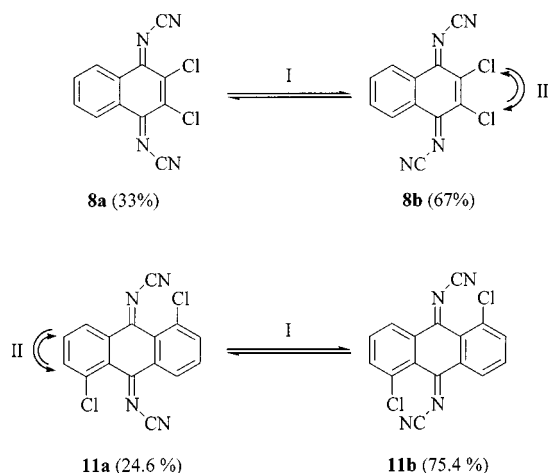


Scheme 3

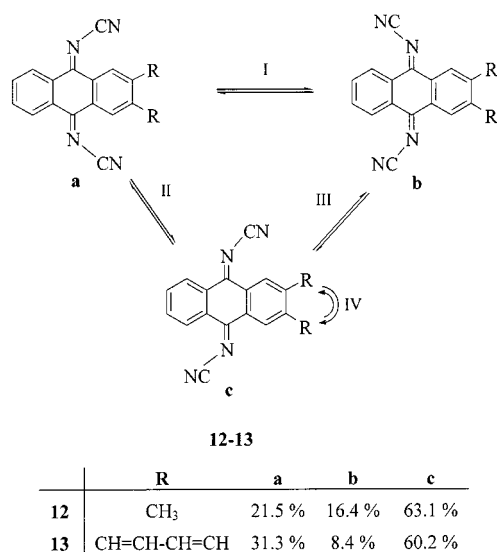
resonances increases, or the chemical shift separation decreases.^[20]

Multisite systems, not amenable to study by conventional methods, can be studied by 2D exchange spectroscopy (2D EXSY). With this method, each single process is separated in the 2D map, so that interferences between processes are avoided.^[21] 2D EXSY has been applied to the resolution of complex kinetic processes, in organometallic chemistry, metallotropy and fluxional behaviour, conformational studies etc.^[22]

A special feature of 2D EXSY is that, rather than the free activation energy, the kinetic constant for each independent process is deduced from the NMR spectral data. More recently, 1D EXSY techniques have been introduced.^[23]



Scheme 4



Scheme 5

Inversion of the cyanoimine group in DCNQIs **6–13** may produce 3–4 isomers with a maximum of four inversion processes and twelve interchange equilibria. This means that, in most cases, it is impossible to find the coalescence temperature for each single process and so is a good example for demonstrating the application of 2D EXSY techniques.

In order to characterize compounds **6–13** when the inversion of the cyanoimine group is a fast process, ¹H NMR spectra at 293 K were recorded. The majority of compounds show broad signals at room temperature as an indication of a kinetic process that is close to coalescence at this temperature (Table 1).

Isomers from each compound were characterized by ¹H NMR in CDCl₃ solution at 223 K (Table 2, Scheme 3–5). At this temperature, inversion of the cyanoimine group is a slow process on the ¹H NMR time scale in all cases.

Identification of isomers was performed considering: i) the anisotropy of the cyano group,^[24] that makes H_{syn} deshielded in relation to H_{anti}; ii) comparison with monoconfigurational compounds; compound **8** (two isomers), for in-

Table 1. NMR spectra of compounds **6–13** at 293 K (δ, ppm, J, Hz, solvent, CDCl₃)

Compound	NMR signals
6	2.34 (s, CH ₃)
7	7.63 (s, H-2, H-3); 7.86 and 8.41 (AA'XX', J _{AA'} = 7.6 Hz, J _{AX} = 7.8 Hz, J _{AX'} = 1.4 Hz, H-6, H-7 and H-5, H-8).
8	7.87 (AA'XX' part AA', J _{AA'} = 7.6 Hz, J _{XX'} = 7.8 Hz, J _{AX'} = 1.5 Hz, H-6, H-7); 8.76 (br. s, H-5, H-8)
9	4.17 (s, OCH ₃); 6.83 (s, H-3); 7.76 and 8.08 (J _{AA'} = 7.5 Hz, J _{XX'} = 7.1 Hz, J _{AX'} = 1.2 Hz, H-6, H-7 and H-5, H-8); 8.93 (s, H-9, H-10)
10	7.66 (t, J = 8 Hz, H-3, H-6); 7.81 (m, H-2, H-7); 9.0–8.4 (br. s, H-4, H-5)
11	7.70 (t, J = 8 Hz, H-3, H-7); 7.80 (d, J = 8.3 Hz, H-2, H-6); 8.35 (br. s, H-4, H-8)
12	2.48 (s, CH ₃); 7.82 (AA'XX' part AA', J _{AA'} = 7.6 Hz, J _{XX'} = 7.8 Hz, J _{AX'} = 1.6 Hz, H-6, H-7); 8.61 (br. s, H-1, H-4); 8.75 (br. s, H-5, H-8)
13	7.80 (m, H-8, H-9); 7.88 (m, H-2, H-3); 8.15 (m, H-7, H-10); 8.4–9.9 (br. s, H-1, H-4, H-6, H-11)

stance, versus compound **7** (one isomer), iii) H,H correlations in the COSY spectra at 223 K; for example in compounds **10**, **11**, **12** (Figure S-1, Supporting Information) and **13**, and iv) the spin system; for example in compounds **8**, **12** and **13**, where symmetrical isomers show an AA'XX' pattern for the benzene ring proton signals while asymmetrical isomers show an ABCD pattern.

Inversion Kinetics by ¹H NMR

Compounds **6**, **7** and **9** reveal only one isomer, represented in Scheme 3 (**6a**, **7a**, **9a**), showing the relative importance of the interaction of the CN group.

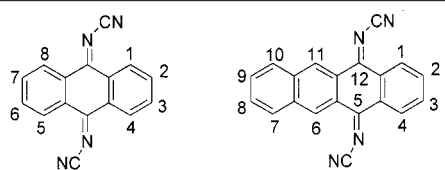
In compound **10**, a monocyanoimine, only one isomer and only one inversion process is possible, represented by the interchange 4-H/5-H. This process can be studied by variable-temperature experiments. The coalescence temperature was found to be 299 K, a value that gives a ΔG[‡] = 13.91 kcal/mol (Scheme 3), very close to the values described for related compounds.^[12]

Compounds **8** and **11** each display two isomers. In both compounds two inversion processes can be detected (processes I and II), represented by three interchanges of 5-H and 8-H in compound **8** and of 4-H and 8-H in compound **11** (Scheme 4).

Finally, compounds **12** and **13** exhibit three isomers, and four inversion processes can be detected (processes I–IV). They are represented by twelve interchange processes, six in each ring fused with the quinone ring. These transformations can be monitored in compound **12** by the interchange of 1-H and 4-H in one ring and 5-H and 8-H in the other ring. Similarly, in compound **13** the inversion can be observed by inspection of the interchange of 1-H and 4-H in one ring and 6-H and 11-H in the other ring (Scheme 5). Figure S-2 (Supporting Information) shows the *peri*-H signal of the EXSY spectrum of compound **13**.

Since in multisite exchange systems it is not possible to detect all processes independently by means of 1D NMR

Table 2. NMR spectra of compounds **8**–**13** at 223 K (δ , ppm, J, Hz, solvent, CDCl₃)

	
Compound ^[a]	NMR signals
8a	7.85 (AA'XX', $J_{AA'} = 7.1$ Hz, $J_{AX} = 7.9$ Hz, $J_{AX'} = 1.4$ Hz, H-6, H-7); 8.31 (AA'XX', H-5, H-8)
8c	7.89 (m, H-7); 7.93 (m, H-6); 8.41 (dd, $J = 7.5, 1.5$ Hz, H-8); 9.19 (dd, $J = 7.5, 1.2$ Hz, H-5)
10	7.66 (t, $J = 8$ Hz, H-6); 7.75 (t, $J = 8$ Hz, H-3); 7.81 (dd, $J = 8, 1.3$ Hz, H-7); 7.86 (dd, $J = 7.9, 1.2$ Hz, H-2); 8.13 (dd, $J = 7.9, 1.3$ Hz, H-5); 8.76 (dd, $J = 7.9, 1.2$ Hz, H-4)
11a	7.66 (t, $J = 7.8$ Hz, H-7); 7.71 (d, $J = 7.5$ Hz, H-3); 7.76 (t, $J = 7.7$ Hz, H-6); 7.81 (m, H-3); 7.99 (dd, $J = 7.5, 1$ Hz, H-8); 8.50 (dd, $J = 6.5, 1.2$ Hz, H-4)
11b	7.73 (t, $J = 8$ Hz, H-3, H-7); 7.83 (dd, $J = 8, 1$ Hz, H-2, H-6); 8.43 (dd, $J = 7.6, 1$ Hz, H-4, H-8)
12a	2.47 (s, CH ₃ -2, CH ₃ -3); 7.77 and 8.25 (AA'XX', $J_{AA'} = 7.5$ Hz, $J_{AX} = 8$ Hz, $J_{AX'} = 1.3$ Hz, H-6, H-7 and H-5, H-8); 8.87 (s, H-1, H-4)
12b	2.40 (s, CH ₃ -2, CH ₃ -3); 7.91 and 9.10 (AA'XX', $J_{AA'} = 7.2$ Hz, $J_{AX} = 7.9$ Hz, $J_{AX'} = 1.1$ Hz, H-6, H-7 and H-5, H-8); 8.01 (s, H-1, H-4)
12c	2.43 (s, CH ₃ -3); 2.45 (s, CH ₃ -2); 7.84 (t, $J = 8$ Hz, H-7); 7.86 (t, $J = 8$ Hz, H-6); 8.14 (s, H-4); 8.38 (dd, $J = 7.9, 1.3$ Hz, H-8); 8.81 (s, H-1); 9.04 (d, $J = 7.8$ Hz, H-5)
13a^[b]	8.37 (AA'XX' part XX', $J_{AA'} = 6.7$ Hz, $J_{AX} = 7.7$ Hz, $J_{AX'} = 1.5$ Hz, H-1, H-4); 9.68 (s, H-6, H-11)
13b^[b]	8.88 (s, H-6, H-11); 9.19 (AA'XX' part XX', $J_{AA'} = 7.5$ Hz, $J_{AX} = 8$ Hz, $J_{AX'} = 1.2$ Hz, H-1, H-4)
13c^[b]	8.51 (dd, $J = 7.5, 1.4$ Hz, H-4); 8.97 (s, H-6); 9.13 (dd, $J = 7.7, 0.9$ Hz, H-1); 9.68 (s, H-11)

^[a] Numbering of the ring systems has been carried out according to the IUPAC rules for aromatic hydrocarbons (rule A-21.2) and the corresponding quinones (rule C-317.1). – ^[a] 2-H, 3-H and 7-H, 8-H, 9-H, 10-H are shown as two multiplets at $\delta = 8.05$ – 8.22 and 7.76 – 8.02 , respectively.

spectra, it is necessary to use DNMR spectra in two dimensions using the EXSY pulse sequence.

The essential feature of a quantitative 2D EXSY experiment is the relationship between the intensity of a cross-peak and the rate constants for chemical exchange. Cross-peaks in the spectrum correspond to nuclei that exchange from one site to another. The intensities of those cross-peaks do not correspond directly to the exchange matrix but to its exponential form.^[21c]

Rate constants can be deduced from the spectrum according to Equation (1)

$$R = -\ln A/\tau_m = -X (\ln \Lambda) X^{-1}/\tau_m$$

where $A_{ij} = I_{ij}/M_j$, τ_m is the mixing time, $I_{ij}(\tau_m)/M_j$ and X is the square matrix of eigenvectors of A_i such that $X^{-1}AX = \Lambda = \text{diag}(\lambda_i)$, with λ_i the i th eigenvalue of A . I_{ij}

can be deduced by measuring the volume of each peak intensity directly from the spectrum. M_j is the volume of the diagonal peak of the spectrum registered with a mixing time close to 0, without any chemical exchange.

An essential feature of the process is that [Equation (2)]

$$K_{ij} p_i = K_{ji} p_j$$

where K_{ij} and K_{ji} are the rate constants of processes $i \rightarrow j$ and $j \rightarrow i$, respectively, and p_i is the relative population of the i th site.

The ΔG^\ddagger values of the inversion processes are collected in Table 3. The energy barrier for the *syn/anti* isomerization of the NCN groups can be estimated from the rate constants and is very close in all compounds: between 13.16 and 13.93 kcal/mol for a single inversion. This value is similar to that obtained for other substituted DCNQIs.^[21,24]

Some isomerizations imply an inversion of two NCN groups. For instance, in compounds **12** and **13**, interconversion of both symmetric isomers implies the inversion of both NCN groups (Scheme 5, process I). The activation free energy increases slightly, to 13.41–14.40 kcal/mol in these cases.

Moreover, self-transformation of some single isomers, e.g. as process IV in Scheme 5, can easily be detected by 2D EXSY spectra. This process again implies a double inversion of the NCN group, for instance in the asymmetric isomers of **8**, **11** (Scheme 4, process II), **12**, and **13** (Scheme 5, process IV). In these processes, the free activation energy again increases to 13.71–15.56 kcal/mol.

Theoretical Calculations

In order to unveil the reasons underlying the experimentally ascertained free energy barriers to isomerization, we performed several calculations on the topomerization of *N*-cyanomethanimine (**14**) at the B3LYP/6–31G* level, both in the gas phase and in solution. Intensive study of the possible transition structures led to the structure **TS**, whose main geometrical features are reported in Figure 1.

This saddle point involves inversion around the iminic nitrogen atom. An alternative transition structure involving rotation around the iminic C=N bond^[25] was not found, since the starting geometries converged to either **14** or **TS** upon optimisation. The main energetic and electronic fea-

Table 3. Activation free energies determined by 2D-EXSY NMR

Compound	Process ^[a]	ΔG^\ddagger [kcal/mol]	ΔG^\ddagger [kJ/mol]
8	8a \rightleftharpoons 8c (I)	13.27 \pm 0.14	55.54 \pm 0.55
8	8c \rightleftharpoons 8c (II)	13.71 \pm 0.12	57.35 \pm 0.51
10	10 \rightleftharpoons 10	13.94 \pm 0.11	58.30 \pm 0.44
11	11a \rightleftharpoons 11b (I)	13.20 \pm 0.31	55.23 \pm 1.31
11	11b \rightleftharpoons 11b (II)	15.56 \pm 0.10	65.11 \pm 0.39
12	12a \rightleftharpoons 12b (I)	14.40 \pm 0.29	60.26 \pm 1.20
12	12a \rightleftharpoons 12c (II)	13.16 \pm 0.17	55.04 \pm 0.73
12	12b \rightleftharpoons 12c (III)	13.31 \pm 0.33	55.69 \pm 1.30
12	12c \rightleftharpoons 12c (IV)	13.76 \pm 0.06	57.55 \pm 0.26
13	13a \rightleftharpoons 13b (I)	13.41 \pm 0.67	56.08 \pm 2.84
13	13a \rightleftharpoons 13c (II)	13.08 \pm 0.34	54.71 \pm 1.90
13	13b \rightleftharpoons 13c (III)	13.04 \pm 0.45	54.55 \pm 1.89
13	13c \rightleftharpoons 13c (IV)	13.93 \pm 0.32	58.27 \pm 1.33

^[a] See Schemes 4–5.

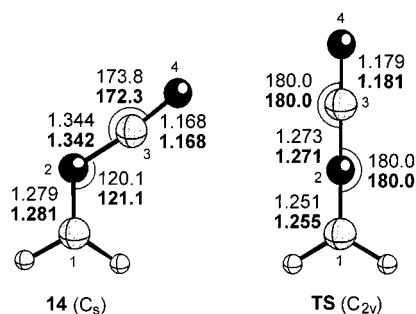


Figure 1. B3LYP/6-31G* (plain text) and B3LYP(LIAl)/6-31G* (chloroform solution, bold text) geometrical data of structures **6a-c**; bond lengths and angles are given in Å and degrees, respectively; in this and in the following figures which include ball-and-stick representations, unless otherwise noted, atoms are represented by increasing depth of shading in the order: H, C, N

tures of the stationary points associated with the topomerization of **14** are collected in Table 4.

Table 4. Activation energies^[a] (ΔE_a , kcal/mol), Gibbs activation energies^[a,b] (ΔG_a , kcal/mol), selected bond indices^[c] (B_{ij} , a.u.), NBA charges^[c] (q_i , a.u.) and dipole moments^[c] (μ , D) associated with topomerization of compound **14**^[d] in the gas phase ($\epsilon = 1.00$) and in chloroform solution^[e] ($\epsilon = 4.81$)

Magnitude	$\varepsilon = 1.00$	$\varepsilon = 4.81$
ΔE_a	14.43	13.30
ΔG_a	14.80	13.67
B₂₃ (14)	1.179	1.193
B₂₃ (TS)	1.302	1.322
B₃₄ (14)	2.776	2.760
B₃₄ (TS)	2.599	2.580
q₂ (14)	-0.471	-0.486
q₂ (TS)	-0.303	-0.485
q₄ (14)	-0.329	-0.374
q₄ (TS)	-0.422	-0.419
μ (14)	4.333	5.163
μ (TS)	4.925	6.178

[a] Computed at the B3LYP/6-31G*+ΔZPVE level. – [b] Computed at 298 K. – [c] Computed at the B3LYP/6-31G* level. – [d] See Figure 1 for atom numbering. – [e] Solvent effects computed using the Onsager–Kirkwood (L1A1) method.

As can be seen, our computed free energy of activation is in very good agreement with our experimental data, particularly if solvent effects are taken into account. This internal coherence between experimental and computational results proves the reliability of both studies and provides additional support to the elegant experiments of Kessler et al.,^[26] that demonstrate that the inversion of imines takes place by inversion mechanisms. Our computational data also explain why the inversion barriers of cyanoimines are relatively low. The natural bonding analysis (NBA)^[27] of **TS** reveals that in this saddle point there is a significant two-electron stabilisation involving the lone pair of the iminic nitrogen atom N2 and the antibonding orbital of the cyano group (Figure 2). The corresponding second-order perturbational energy is calculated to be -79.42 kcal/mol at the B3LYP(L1A1)/6-31G* level.

This very large value is due in part to the favourable orientation between the sp-hybridized N2 atom and the cyano moiety. For instance, in compound **14** the same two-elec-

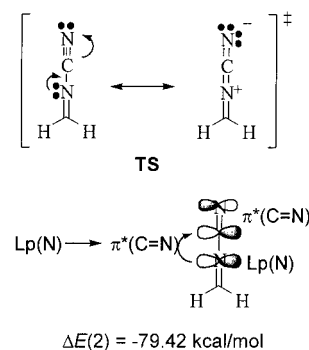


Figure 2. Main resonance forms and two-electron interaction in structure **TS** computed at the B3LYP/6-31G* level

tron interaction is calculated to be only -12.27 kcal/mol. Therefore, the resonance shown in Figure 2 promotes larger bond indices for the N2–C3 bonds of **TS** with respect to **14**. The computed charges on the N2 and N4 atoms in **TS** and **14** are also in agreement with this analysis (Table 4). Another important consequence of this resonance is that **TS** is more polar than **14**, as reflected in the larger dipole moments reported in Table 4. Therefore, the activation barriers computed in solution are lower than those found in the gas phase.

As support for the experimental determinations, the molecular structure of all isomers of compounds **6–13** were investigated by means of the semiempirical methods AM1 and PM3.^[28] In some cases (compounds **6** and **8**, see below), ab initio methods^[29] HF/3–21G* and HF/6–31G* have also been included. The chief geometric features of the structures **6a–c** and **8a–c** are shown in Figures S-3 and S-4 (Supporting Information), respectively. The reported data correspond to those obtained at the B3LYP(L1A1)/6–31G* level in chloroform solution ($\epsilon = 4.81$, vide infra). In any case, the gas-phase geometries obtained at the B3LYP/6–31G* level are very similar to those found in solution.

With other DCNQI derivatives,^[17,18] semiempirical calculations indicate that, in all compounds studied, the molecule adopts a butterfly shape with the central DCNQI ring in a boat conformation. Hence, the steric interactions between the cyano groups and atoms in *peri* (or *ortho*) positions are avoided.

In all isomers of compound **13** the difference in stability between the planar and butterfly-type structure is around 9 kcal (see Table S-3, Supporting Information), indicating a clear preference for this latter geometry, as calculations and X-ray crystallographic data have shown for related compounds.^[18] Deviations from planarity calculated for **13** are similar to those observed from X-ray analysis.

On the other hand, in compound **7**, AM1 calculations indicate that the boat structure should be more stable than the planar by a few calories. Nevertheless, analogous compounds, as well as compound **12**,^[15] have been shown to be planar by X-ray.^[16] So, in order to gain a deeper insight

into the geometry of these compounds and the validity of semiempirical methods, we have fully optimised the molecular geometry of compounds **6** and **8** by using SCF–MO and DFT methods.

The deviations from planarity for isomers **a–c** of compounds **6** and **8**, calculated by means of different methods, are collected in Table S-4 (Supporting Information).

It is interesting to note that at the B3LYP/6–31G* level the geometries for **6a** and **8a,c** are predicted to be planar, in particular when solvent effects are taken into account. This result is in agreement with the experimental evidence. In contrast, AM1 and PM3 predict uniformly butterfly structures. An examination of the main two-electron interaction computed on the natural bonding orbital (NBO) basis provides an explanation for the preference for planar structures. According to natural bonding analysis (NBA, vide infra), an important stabilising factor in the conjugated structures **6a–c** and **8a–c** consists of the donation from the endocyclic $\pi(\text{C}=\text{C})$ NBO to the exocyclic antibonding $\pi^*(\text{C}=\text{N})$ NBO. For instance, in **6a** the second-order energy associated with this stabilising two-electron interaction is calculated to be -22.08 kcal/mol at the B3LYP(L1A1)/6–31G* level^[27] (see Figure S-5A, Supporting Information). However, the same interaction in the butterfly-shaped structure of **6a** computed on the geometry is only -15.91 kcal/mol at the same level. Therefore, although electrostatic arguments favour butterfly structures because of the repulsion between the C–Cl and CN dipoles, stereoelectronic effects favour the planar structures. It is also noteworthy that in all structures the NCN angles of the cyanoimine moieties are not planar. In all cases, the computed departure from linearity is of ca. 10° (Figures S-3 and S-4, Supporting Information). This effect is due mainly to the donation from the lone pairs (Lps) of the sp^2 -hybridized nitrogen atoms to the $\pi^*(\text{C}=\text{N})$ NBOs. For instance, in **6a** it is found that the second-order energy associated with the $\text{Lp}(\text{N}) \rightarrow \pi^*(\text{C}=\text{N})$ interaction is -31.8 kcal/mol (see Figure S-5B, Supporting Information). A similar effect has been found in other nitrogen-containing cumulenes such as isocyanates.^[30] In addition, in structures **6a,c** and **8a,c** there are two-electron donations from the lone pair of the chlorine atom to the $\pi^*(\text{C}=\text{N})$ NBO, with associated energies of ca. 2–3 kcal/mol (for instance, see Figures S-5C and S-6A, Supporting Information). These latter stabilising interactions are also related to the relative energies of the different stereoisomers (vide infra).

The relative energies of structures **6a–c** and **8a–c** at different computational levels are reported in Table 5; the energies for the same compounds are collected in Table S-3 (Supporting Information). From these results it can be concluded that AM1 gives better relative energies than PM3 in these systems, since the computed relative stabilities are in better agreement with the experimental results. However, these results must be considered with caution, given the uniform preference for butterfly structures in this semiempirical Hamiltonian. The B3LYP calculations yield good results, particularly when solvent effects are taken into account. From our results at the B3LYP/6–31G* level and

Table 5. Relative energies, in kcal/mol calculated for isomers **a–c** of compounds **6** and **8** by using different methods

Method	6a	6b	6c	8a	8b	8c
PM3	0.00	−0.73	−0.55	0.00	−0.89	−0.62
AM1	0.00	+1.32	+0.66	0.00	+1.53	+0.67
HF/3–21G(*)	0.00	+2.10	+0.63	0.00	+0.62	−0.16
HF/6–31G*	0.00	−0.31	−0.43	0.00	−2.96	−1.64
HF(L1A1)/6–31G*	0.00	+0.51	−0.11	0.00	−0.79	+0.31
B3LYP/6–31G*	0.00	+1.40	+0.35	0.00	−0.74	−0.57
B3LYP(L1A1)/6–31G*	0.00	+2.14	+0.89	0.00	+0.41	+0.04

the NBA, **6a** is the most stable structure in the case of compound **6**. This result is due to the stabilising $\text{Lp}(\text{Cl}) \rightarrow \pi^*(\text{C}=\text{N})$ interactions in **6a**. In **6c** there is only one interaction of this type, thus resulting in a relatively higher energy. In addition, although the intramolecular electrostatic interaction between the CN and C–Cl dipoles is destabilising, the intermolecular solvation energy is larger, since the electrostatic part of the solvation energy is proportional to the square of the molecular dipole moment in the Onsager–Kirkwood model (vide infra). Therefore, both stereoelectronic and solvent effects favour the stabilisation of structure **6a**.

In the case of compound **8**, aside from the $\text{Lp}(\text{Cl}) \rightarrow \pi^*(\text{C}=\text{N})$ interaction, there are $\text{C}(\text{sp}^2)\text{–H}$ bonds coplanar with the CN moieties. The average distance between these hydrogen atoms and the sp -hybridised carbon atom of the closest cyano group is ca. 2.25 Å (see Figure S-4, Supporting Information). Therefore, since C–H bonds can act as efficient donors,^[31] these interactions can partially stabilise structures **8b,c**. For example, in **8c** the $\sigma(\text{C–H}) \rightarrow \pi^*(\text{C}=\text{N})$ donation is calculated to be quite similar to that associated with the $\text{Lp}(\text{Cl}) \rightarrow \pi^*(\text{C}=\text{N})$ interaction (Figure S-6, Supporting Information). As a consequence, the stereoelectronic, Coulombic and solvent effects are comparable and the relative energies of isomers **8a** and **8c** are quite similar at the B3LYP(L1A1)/6–31G* level, in good agreement with the experimental evidence.

In Table S-4 (Supporting Information) we have also included the Boltzmann populations of compounds **6–13**, computed at 293 K and using the AM1 method. The general trends are in qualitative agreement with the preceding discussion and with the experimental data. However, it must be noted that a higher theoretical level is required to obtain quantitative concordance with those obtained in our NMR analysis (vide supra).

Conclusions

Low-temperature NMR spectra and 2D EXSY experiments have proved to be a valuable tool to study the inversion of the cyanoimine group in DCNQI derivatives. The structures of all isomers have been determined, their NMR spectra have been assigned and the thermodynamic parameters of the inversion of the cyanoimine group have been calculated.

The validity of this methodology for evaluation of rate constants and free activation energy of the NCN group of DCNQIs can be confirmed by: i) comparison of the calculated ΔG^\ddagger values with previously reported values and with computational studies (these studies demonstrate that the isomerization process involves inversion of the imine nitrogen atom and not rotation around the imine C=N bond),^[12,16,18] ii) considering compound **12** where comparison of the calculated ΔG^\ddagger by determination of the coalescence temperature and 2D EXSY experiments show an excellent agreement (13.91 versus 13.94 kcal/mol), and iii) by a good agreement with the semiempirical calculations. However, considering the minor isomers, no linear relation between differences in energy and differences in the isomers ratio was found.

Semiempirical and ab initio calculations have supported the experimental determinations and have permitted the elucidation of the conformation of DCNQI derivatives and the origin of the differential stability of isomers.

Comparison of semiempirical and DFT calculations have shown that, for these systems, AM1 appears to be the method of choice in larger systems whose size precludes energy calculations at more sophisticated levels.

The following structural conclusions can be drawn. Firstly, DCNQI rings adopt a boat conformation in order to avoid steric interactions between the cyano group and the atom in the *peri* (or *ortho*) position. Secondly, NBA shows that donation of the endocyclic $\pi(\text{C}=\text{C})$ NBO to the exocyclic antibonding $\pi^*(\text{C}=\text{N})$ NBO is responsible for the higher stability of planar structures in compounds **6** and **8**. Thirdly, donation from the Lps of the sp^2 -hybridized nitrogen atoms to the $\pi^*(\text{C}=\text{N})$ NBOs explains the nonplanarity of the NCN angles of the cyanoimine moieties. Fourthly, stabilising $\text{Lp}(\text{Cl}) \rightarrow \pi^*(\text{C}=\text{N})$ and $\sigma(\text{C}-\text{H}) \rightarrow \pi^*(\text{C}=\text{N})$ interactions are responsible for the greater stabilisation of structures **6a** and **8c**.

Experimental Section

NMR Studies: NMR spectra were recorded with a Varian Unity 300 spectrometer operating at 299.980 MHz for ^1H . Spectra were recorded at the indicated temperature (± 0.1 K) with a probe calibrated with methanol. The standard Varian pulse sequence was used (VNMR 5.3 software, COSY and NOESY pulse sequences). Samples were prepared dissolving the cyanoimine (0.05 mmol) in CDCl_3 (0.6 mL) under argon. – ^1H , ^1H COSY spectra were acquired using a 1-kHz spectral width; 4 transients of 256 data points were collected for each $256 t_1$ increments. A 1-s relaxation delay, a 10.8-s (45°) pulse width and a 0.125-s acquisition time were used. The data were processed using zero filling and sine-bell functions in both dimensions before Fourier transformation. – The 2D exchange spectra (EXSY) were acquired in the phase-sensitive mode using the States–Haberkorn method.^[32] Typically, a 1-kHz spectral width, 16 transients of 256 data points were collected for each $256 t_1$ increments. A 0.2-s relaxation delay, a 21.5-s (90°) pulse width and a 0.125-s acquisition time were used. The free induction decays were processed with square cosine-bell filters in both dimensions and zero filling was applied prior to double Fourier transformation. – Determination of the kinetic parameters required two experi-

ments with mixing times of 1 s (optimised) for the exchange experiment and 0.05 s for the nonexchange spectra, respectively. The cross peak/diagonal ratio was determined by integrating the volume under the peaks.

Free energy of activation for compound **10** was calculated from the coalescence temperature, determined to ± 1 K, and the frequency difference between the coalescing signals with the formula $\Delta G^\ddagger = aT(10.319 + \log T/\delta\nu)$.^[19b] The estimated error in the calculated free energy is 1.0 kJmol^{-1} .

Computational Methods: The molecular geometry of compounds **6** and **8** were fully optimised using semiempirical and ab initio methods.

Semiempirical calculations were carried out with the AM1^[33] Hamiltonian with standard parameters^[33,34] as implemented in the MOPAC 6.0 package.^[35] All stationary points were refined by minimisation of the gradient norm of the energy at least below 0.01 kcal/Å, deg and characterised by harmonic vibrational frequency analysis.

All ab initio calculations were performed using the GAUSSIAN 94^[29] suite of programs, with the 3–21G(*) and 6–31G* basis set.^[36] Geometry optimisations were carried out at the Hartree–Fock level of theory and were further optimised using density functional theory^[37] (DFT). For this purpose, we used the hybrid three parameters functional developed by Becke and usually denoted as B3LYP.^[38] This method combines Becke's gradient-corrected exchange functional and the Lee–Yang–Parr and Volko–Wilk–Nusair correlation functional^[39] with part of the exact Hartree–Fock exchange energy. Zero-point vibrational energies (ZPVE) were scaled by 0.89^[40] when computed at the HF/3–21G(*) and 6–31G* levels. Stationary points were characterised by frequency calculations.^[41]

We studied the geometry of these compounds not only in vacuo but also in the presence of CHCl_3 ($\epsilon = 4.81$) as organic solvent. The electrostatic contribution of the solution energy was estimated by means of the Onsager method,^[42] denoted as LIA1.^[43] The Onsager reaction field method has been implemented^[44] in the GAUSSIAN 94 series of programs.

Bond orders^[45] and atomic charges^[46] were calculated with the natural bond orbital (NBO) method.^[47] Donor-acceptor interactions were also computed by means of the NBO model.

Preparation of DCNQI Derivatives: Compounds **7**, **8**, **11** and **12** were prepared according to Hünig's procedure.^[12] Compound **6**,^[48] compound **9**,^[49] and compound **13**^[50] were prepared by following the methods previously reported.

1,8-Dichloro-*N*-cyano-9,10-anthraquinon-10-imine (10): To a solution of 1,8-dichloro-9,10-anthraquinone (2 mmol) in dry CH_2Cl_2 (50 mL) at room temperature and under argon, were added dropwise TiCl_4 (0.4 mL, 4.2 mmol) followed by BTC (0.94 mL, 3.5 mmol). The reaction mixture was stirred for 24 h. Then, CH_2Cl_2 (200 mL) was added and the mixture was poured into ice/water (200 mL). The reaction mixture was vigorously stirred until the solution reached room temperature. The organic phase was separated and washed with plenty of water, dried with MgSO_4 and concentrated to 10 mL. The same volume of hexane (10 mL) was added and a solid precipitated. This was collected by filtration and washed with hexane; 47% yield; m.p. 218–219 °C. – ^1H NMR (300 MHz, CDCl_3): $\delta = 7.66$ (t, $J = 8.0$ Hz, 2-H, 7-H), 7.81 (m, 3-H, 6-H), 9.0–8.4 (br. s, 4-H, 5-H). – ^{13}C NMR (75 MHz, CDCl_3): $\delta = 113.1, 125.5, 126.1, 132.2, 134.7, 136.4, 137.7, 170.0$. – IR (KBr): $\tilde{\nu} = 2195, 1700, 1605, 1580, 1560, 1455, 1340, 1250$,

1195, 1150, 840, 800, 720 cm^{-1} . – MS (EI); m/z (%): 300 (100) $[\text{M}^+]$. – $\text{C}_{15}\text{H}_6\text{Cl}_2\text{N}_2\text{O}$: calcd. C 59.83, H 2.01, N 9.30; found C 59.94, H 2.48, N 9.20.

Acknowledgments

This work was supported by the Spanish DGESIC (Grants PB97-0429, PB96-1481 and PB98-0818) and by the Basque Government (Grant EX1998-126).

- [1] [1a] *Charge-Transfer Salts, Fullerenes and Photoconductors*, vol. 1 in: *Handbook of Organic Conductive Molecules and Polymers* (Ed.: H. S. Nalwa), John Wiley & Sons Ltd., 1997. – [1b] Special Issue on Molecular Conductors, *J. Mater. Chem.* **1995**, *5*, 1469. – [1c] *Organic Conductors – Fundamentals and Applications* (Ed.: J. P. Farges), Marcel-Dekker, New York, 1994. – [1d] J. M. Williams, J. R. Ferraro, R. J. Thorn, K. D. Carlsson, U. Geiser, H. H. Wang, A. M. Kini, M. H. Whangho, *Organic Superconductors (including Fullerenes)*, Prentice Hall, 1992. – [1e] M. R. Bryce, *Chem. Soc. Rev.* **1991**, *20*, 355–390.
- [2] M. R. Bryce, L. C. Murphy, *Nature* **1984**, *309*, 119–121.
- [3] L. R. Melby, R. J. Harder, W. R. Hertler, W. Mahler, R. E. Benson, W. E. Mochel, *J. Am. Chem. Soc.* **1962**, *84*, 3374–3387.
- [4] A. Aumüller, S. Hünig, *Angew. Chem.* **1984**, *96*, 437–438; *Angew. Chem. Int. Ed. Engl.* **1984**, *23*, 447–448.
- [5] For a review, see: P. Cassoux, L. Valade, in *Molecular Inorganic Superconductors in Inorganic Materials* (Eds.: D. W. Bruce, D. O'Hare), Wiley, New York, 1992.
- [6] [6a] N. Martín, L. Sánchez, B. Illescas, I. Pérez, *Chem. Rev.* **1998**, *98*, 2527–2548. – [6b] L. Echegoyen, L. E. Echegoyen, *Acc. Chem. Res.* **1998**, *31*, 593–601. – [6c] A. Hirsch, in *The Chemistry of Fullerenes*, Georg Thieme, Stuttgart, 1994.
- [7] For a recent review, see: N. Martín, J. L. Segura, C. Seoane, *J. Mater. Chem.* **1997**, *7*, 1661–1676.
- [8] For a recent review, see: T. Nakuyama, in *Electrically Conductive Langmuir–Blodgett Films*, chapter 14, vol. 1 in *Handbook of Organic Conductive Molecules and Polymers* (Ed.: H. S. Nalwa), John Wiley & Sons Ltd., 1997.
- [9] [9a] M. C. Grossed, S. C. Weston, *Contemp. Org. Chem.* **1994**, 367–384. – [9b] *Introduction to Molecular Electronics* (Eds.: M. C. Petty, M. R. Bryce, D. Bloor), Oxford University Press, New York, 1995. – [9c] See also: R. A. Janssen, P. T. Christians, C. Hare, N. Martín, N. S. Saricifti, A. J. Heeger, F. Wudl, *J. Chem. Phys.* **1995**, *103*, 8840–8845.
- [10] [10a] J. Ferraris, D. O. Cowan, V. V. Walatka, J. M. Perlstein, *J. Am. Chem. Soc.* **1973**, *95*, 948–949. – [10b] L. B. Coleman, M. J. Cohen, A. J. Sandman, F. G. Yamagishi, A. F. Garito, A. J. Heeger, *Solid State Commun.* **1973**, *12*, 1125–1128.
- [11] For some reviews, see: [11a] S. Hünig, P. Erk, *Adv. Mater.* **1991**, *3*, 225–236. [11b] S. Hünig, *J. Mater. Chem.* **1995**, *5*, 1469–1479.
- [12] A. Aumüller, S. Hünig, *Liebigs Ann. Chem.* **1986**, 142–164.
- [13] A. Aumüller, S. Hünig, *Liebigs Ann. Chem.* **1986**, 165–176.
- [14] N. Martín, C. Seoane, in *From Electron Acceptor Molecules to Photoinduced Intramolecular Electron-Transfer Systems*, chapter 1 in *Handbook of Organic Conductive Molecules and Polymers* (Ed.: H. S. Nalwa), John Wiley & Sons Ltd., 1997.
- [15] U. Schubert, S. Hünig, A. Aumüller, *Liebigs Ann. Chem.* **1985**, 1216–1222.
- [16] [16a] P. Erk, S. Hünig, G. Klebe, T. Metzenthin, H. P. Werner, J. H. von Schütz, *Liebigs Ann./Recueil* **1997**, 1235–1243. – [16b] S. Hünig, R. Bau, M. Kemmer, H. Meixner, T. Metzenthin, K. Peters, K. Sinzger, J. Gulbis, *Eur. J. Org. Chem.* **1998**, 335–348. – [16c] S. Hünig, K. Sinzger, M. Kemmer, U. Lagohr, H. Rieder, S. Söderholm, J. U. Schütz, H. C. Wolf, *Eur. J. Org. Chem.* **1998**, 1977–1988.
- [17] B. Illescas, N. Martín, J. L. Segura, C. Seoane, E. Ortí, P. M. Viruela, R. Viruela, *J. Mater. Chem.* **1995**, *5*, 1563–1570.
- [18] N. Martín, J. L. Segura, C. Seoane, E. Ortí, P. M. Viruela, R. Viruela, A. Albert, F. H. Cano, J. Vidal-Gancedo, C. Rovira, J. Veciana, *J. Org. Chem.* **1996**, *61*, 3041–3054.
- [19] [19a] H. Günther, in *NMR Spectroscopy, Basic Principles, Concepts and Applications in Chemistry*; 2nd ed., chapter 9, John Wiley & Sons, 1992, p. 336. – [19b] J. Sandström, in *Dynamic NMR Spectroscopy*, Academic Press, New York, 1982.
- [20] J. Noggle, R. Schirmer, in *The Nuclear Overhauser Effect*, Academic Press, New York, 1972.
- [21] [21a] C. L. Perrin, R. K. Gipe, *J. Am. Chem. Soc.* **1984**, *106*, 4036–4038. – [21b] J. Bremer, G. L. Mendz, W. J. Moore, *J. Am. Chem. Soc.* **1984**, *106*, 4691–4696. – [21c] C. L. Perrin, T. J. Dwyer, *Chem. Rev.* **1990**, *90*, 935–967.
- [22] See for instance: [22a] A. Gogoll, J. Örnebro, H. Greenberg, J. E. Bäckvall, *J. Am. Chem. Soc.* **1994**, *116*, 3631–3632. – [22b] A. Gelling, M. D. Olsen, K. G. Orrell, A. G. Osborne, V. Šik, *Chem. Commun.* **1997**, 587–588. – [22c] D. J. Ma, J. Lu, J. Hu, W. X. Tang, *Spectrosc. Lett.* **1998**, *31*, 727–736. – [22d] A. Soi, W. Bauer, H. Mauser, C. Moll, F. Hampel, A. Hirsch, *J. Chem. Soc., Perkin Trans. 2* **1998**, 1471–1478. – [22e] A. Fletcher, B. G. Gownlock, K. G. Orrell, *J. Chem. Soc., Perkin Trans. 2* **1998**, 797–803. – [22f] H. Gehring, E. Dal Trozzo, *Helv. Chim. Acta* **1998**, *81*, 236–250.
- [23] C. L. Perrin, R. E. Engler, *J. Am. Chem. Soc.* **1997**, *119*, 585–591.
- [24] P. Bando, N. Martín, J. L. Segura, C. Seoane, E. Ortí, P. M. Viruela, R. Viruela, A. Albert, F. H. Cano, *J. Org. Chem.* **1994**, *59*, 4618–4629.
- [25] E. Eliel, S. H. Wilen, *Stereochemistry of Organic Compounds*, Wiley, New York, 1994, p. 550–555.
- [26] [26a] H. Kessler, D. Leibfritz, *Chem. Ber.* **1971**, *104*, 137. – [26b] H. O. Kalinowski, H. Kessler, *Top. Stereochem.* **1973**, *7*, 295.
- [27] For a brief discussion on the reliability of NBA within the DFT framework, see: A. Arrieta, B. Lecea, F. P. Cossio, *J. Org. Chem.* **1998**, *63*, 5869–5876.
- [28] Calculated with the help of Hyperchem 5.1: Autodesk.
- [29] Calculated with the help of Gaussian 94 (Revision A.1): M. J. Frisch, G. W. Trucks, H. B. Schlegel, P. M. W. Gill, B. G. Johnson, M. A. Robb, J. R. Cheeseman, T. A. Keith, G. A. Petersson, J. A. Montgomery, K. Raghavachari, M. A. Al-Laham, Zakrzewski, J. V. Ortiz, J. B. Foresman, C. Y. Peng, P. Y. Ayala, M. W. Wong, J. L. Andres, E. S. Replogle, R. Gomperts, R. L. Martin, D. J. Fox, J. S. Binkley, D. J. Defrees, J. Baker, J. P. Stewart, M. Head-Gordon, C. Gonzalez, J. A. Pople, Gaussian, Inc., Pittsburgh PA, 1995.
- [30] G. Roa, J. M. Ugalde, F. P. Cossio, *J. Phys. Chem.* **1996**, *100*, 9619–9623.
- [31] [31a] A. S. Cieplak, B. D. Tait, C. R. Johnson, *J. Am. Chem. Soc.* **1989**, *111*, 8447–8462. – [31b] B. Lecea, A. Arrieta, F. P. Cossio, *J. Org. Chem.* **1997**, *62*, 6485–6492. – [31c] B. Lecea, A. Arrieta, F. P. Cossio, *J. Org. Chem.* **1998**, *63*, 5216–5227.
- [32] D. J. States, R. A. Haberkorn, D. J. Ruben, *J. Magn. Reson.* **1982**, *48*, 286–292.
- [33] M. J. S. Dewar, E. G. Zoebisch, E. F. Healy, J. J. P. Stewart, *J. Am. Chem. Soc.* **1985**, *107*, 3902–3909.
- [34] M. J. S. Dewar, E. G. Zoebisch, *Theochem* **1988**, 180.
- [35] [35a] J. J. P. Stewart, *QCPE Bull.* **1983**, *3*, 101. – [35b] Indiana University, Bloomington, IN, *QCPE*, No. 455.
- [36] W. J. Hehre, L. Radom, P. R. Schleyer, J. A. Pople, *Ab initio Molecular Orbital Theory*, Wiley, New York, 1986, p. 65–88 and references therein.
- [37] R. G. Parr, W. Yang, *Density-Functional Theory of Atoms and Molecules*, Oxford, New York, 1989.
- [38] A. D. Becke, *J. Chem. Phys.* **1993**, *98*, 5648–5652.
- [39] [39a] A. D. Becke, *Phys. Rev. A* **1988**, *38*, 3098. – [39b] C. Lee, W. Yang, R. G. Parr, *Phys. Rev. B* **1980**, *37*, 785. – [39c] S. H. Vosko, L. Wilk, M. Nusair, *Can. J. Phys.* **1980**, *58*, 1200.
- [40] J. A. Pople, B. Schleyer, R. Krishnan, D. J. DeFrees, J. S. Binkley, H. Frisch, R. Whiteside, R. F. Hout, W. J. Herhe, *Int. J. Quantum Chem. Symp.* **1981**, *15*, 269.
- [41] J. W. McIver, A. K. Komornicki, *J. Am. Chem. Soc.* **1972**, *94*, 2625–2633.
- [42] L. Onsager, *J. Am. Chem. Soc.* **1936**, *58*, 1486–1493.
- [43] I. Morao, B. Lecea, A. Arrieta, F. P. Cossio, *J. Am. Chem. Soc.* **1997**, *119*, 816–825.
- [44] [44a] O. Tapia, O. Goscinski, *Mol. Phys.* **1975**, *29*, 1953. – [44b] M. W. Wong, K. B. Wiberg, *J. Chem. Phys.* **1991**, *95*, 8991–8998. – [44c] M. W. Wong, K. B. Wiberg, *J. Am. Chem. Soc.* **1991**, *113*, 4776–4782.
- [45] K. B. Wiberg, *Tetrahedron* **1968**, *24*, 1083–1096.

- [46] K. B. Wiberg, P. R. Rabien, *J. Comput. Chem.* **1993**, *14*, 1504.
- [47] [47a] A. E. Reed, R. B. Weinstock, F. Weinhold, *J. Chem. Phys.* **1985**, *83*, 735–746. – [47b] A. E. Reed, L. A. Curtiss, F. Weinhold, *F. Chem. Rev.* **1988**, *88*, 899–926.
- [48] N. Martín, J. L. Segura, C. Seoane, C. Torío, A. González, J. M. Pingarrón, *Synth. Met.* **1994**, *64*, 83–89.
- [49] E. Barranco, N. Martín, J. L. Segura, C. Seoane, P. de la Cruz, F. Langa, A. González, J. M. Pingarrón, *Tetrahedron* **1993**, *49*, 4881–4892.
- [50] N. Martín, J. A. Navarro, C. Seoane, A. Albert, F. H. Cano, J. Y. Becker, V. Khodorkovsky, E. Harlev, M. Hanack, *J. Org. Chem.* **1992**, *57*, 5726–5730.

Received December 17, 1999
[O99676]